Parity-time-symmetric optoelectronic oscillator based on higher-order optical modulation

Qiao, Yu; Zhang, Yu; Zheng, Ruiqi; Chan, Erwin H.W.; Wang, Xudong; Feng, Xinhuan; Guan, Bai Ou; Yao, Jianping

Published in:
Optics Letters

DOI:
10.1364/OL.469634

Published: 01/09/2022

Document Version
Peer reviewed version

A parity-time-symmetric optoelectronic oscillator based on higher order optical modulation

YU QIAO,[1] YU ZHANG,[1] RUIQI ZHENG,[1] ERWIN H. W. CHAN,[2] XUDONG WANG,[1,*] XINHUAN FENG,[1] BAI-OU GUAN,[1] AND JIANPING YAO[1,3]

[1]*Institute of Photonics Technology, Jinan University, Guangzhou 510632, China*
[2]*College of Engineering, IT and Environment, Charles Darwin University, Darwin NT 0909, Australia*
[3]*School of Electrical Engineering and Computer Science, University of Ottawa, K1N 6N5, Ontario, Canada*
**Corresponding author: txudong.wang@email.jnu.edu.cn*

Received 3 July 2022; revised XX Month, XXXX; accepted XX Month XXXX; posted XX Month XXXX (Doc. ID XXXXX); published XX Month XXXX

An optoelectronic oscillator (OEO) for single-frequency microwave generation enabled by broken parity time (PT) symmetry based on higher order modulation using a Mach-Zehnder modulator is proposed and demonstrated. Instead of using two physically separated mutually coupled loops with balanced gain and loss, the PT symmetry is realized using a single physical loop to implement two equivalent loops with the gain loop formed by the beating between the optical carrier and the ±1st order sidebands and the loss loop formed by the beating between the ±1st order sidebands and the ±2nd order sidebands at a photodetector. The gain and loss coefficients are made identical in magnitude by controlling the incident light power to the modulator and the modulator bias voltage. Once the gain/loss coefficient is greater than the coupling coefficient, the PT symmetry is broken and a single-frequency oscillation without using an ultra-narrow passband filter is achieved. The approach is evaluated experimentally. For an OEO with a loop length of 10.1 km, a single-frequency microwave signal at 9.997 GHz with a 55 dB sidemode suppression ratio and -142 dBc/Hz phase noise at a 10 kHz offset frequency is generated. No mode hopping is observed during a 5-hour measurement period. © 2022 Optical Society of America

http://dx.doi.org/10.1364/OL.XX

An optoelectronic oscillator (OEO) is a hybrid feedback system consisting of an optical path and an electrical path, which can be used to generate a low-phase-noise microwave signal thanks to the high Q factor offered by the low-loss optical path [1]. However, an OEO with a long fiber in the loop will produce a large number of closely spaced longitudinal modes due to a very small free spectral range (FSR). For example, the mode spacing of an OEO with a loop length of 10 km is only 20 kHz, which is very small, and a microwave bandpass filter (BPF) cannot have a very narrow bandwidth to perform single mode selection.

A technique that employs dual loops with one having a long length and the other a short length with a large equivalent FSR but still maintaining a large Q factor, known as the Vernier effect [2], has been proposed for single mode selection. The use of injection locking [3] can also enable single mode selection. However, the approaches based on a dual loop structure or using injection locking make the system complicated. Recently, parity time (PT) symmetry, a concept resulted originally from quantum mechanics, has been introduced to microwave photonics for mode selection. An OEO employing PT symmetry will have a strongly enhanced gain difference between the dominant mode and the side modes, simplifying mode selection without the need of an ultra-narrow microwave BPF [4]. To realize PT symmetry in an OEO, two mutually coupled loops with one having a gain and the other a loss with the gain and loss coefficients identical in magnitude are needed. The two loops can be implemented using two spatially distributed subspaces, such as two resonators [5], [6], or a single spatial resonator with two equivalent loops in the wavelength space [7] or polarization space [8]. A PT symmetric OEO implemented using a single spatial resonator has the advantage of simple structure, which can not only reduce the system cost but also make the system have better stability. However, the PT symmetric OEOs reported in [7] and [8] are implemented using two wavelengths or two polarization states. To further simplify the system a single wavelength or a single polarization state may be used.

In this paper, we propose and experimentally demonstrate a new PT symmetric OEO in a single physical loop using a single wavelength with one polarization, in which the two equivalent loops are implemented based on high order intensity modulation using a Mach-Zehnder modulator (MZM). The operation of the OEO is evaluated experimentally. For an OEO with a loop length of 10.1 km, stable single-frequency oscillation is achieved. A microwave signal at 9.997 GHz with a high sidemode suppression ratio of 55 dB and an ultra-low phase noise of -142 dBc/Hz at a 10 kHz offset frequency is generated.

The schematic of the PT symmetric OEO based on higher order modulation is shown in Fig. 1. A continuous wave (CW) light generated by a laser diode (LD) is launched into a MZM via a polarization controller (PC). The modulated signal is sent through a long dispersion shifted fiber (DSF) and applied to a photodetector (PD). An electronic amplifier (EA) is connected to the PD and the amplified signal is filtered by a microwave BPF and then applied to the MZM to close the

OEO loop. Note that the use of a DSF rather than a standard single-mode fiber (SMF) is to reduce the chromatic dispersion, which may make the two equivalent loops have different time delays, which will fail the PT symmetry.

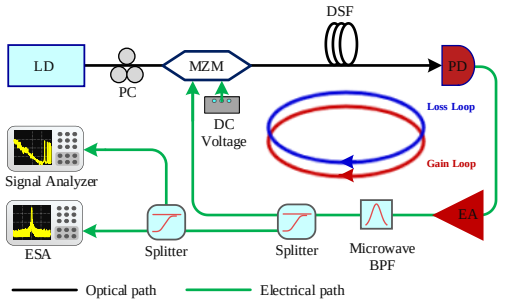

Fig. 1. Schematic of the proposed PT symmetric OEO. The red circle indicates an RF signal travelling in the feedback loop formed by the beating between the optical carrier and the ±1st order sidebands at the PD. The blue circle indicates an RF signal travelling in the feedback loop formed by the beating between the ±1st order sidebands and the ±2nd order sidebands at the PD. EA: electronic amplifier, LD: laser diode, MZM: Mach-Zehnder modulator, PC: polarization controller.

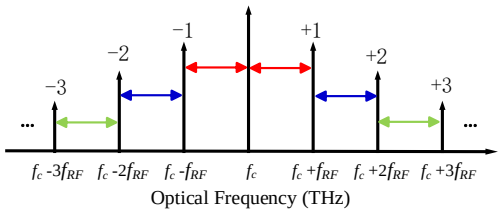

Fig. 2. The optical spectrum at the output of the MZM, where f_c and f_{RF} are the optical carrier frequency and the input RF signal frequency, respectively.

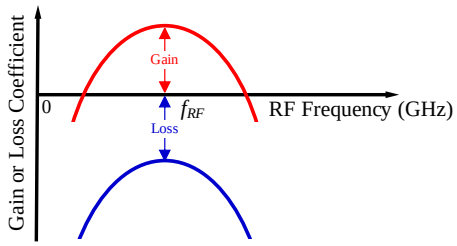

Fig. 3. The gain and loss coefficients versus RF signal frequency.

Figure 2 shows the optical spectrum at the output of the MZM. As can be seen, in addition to the optical carrier and the ±1st order sidebands, the higher order sidebands are generated due to the higher order modulation. The beating between the optical carrier and the ±1st order sidebands at the PD will generate a photocurrent at the fundamental RF signal frequency f_{RF}. The beating between the ±1st order sidebands and the ±2nd order sidebands at the PD will also generate a photocurrent at the same frequency f_{RF}. As can be seen from Fig. 1, the RF signals at the output of the PD are fed back to the MZM. This shows that there exist two equivalent feedback loops, with the gain loop formed by the beating between the optical carrier and the ±1st order sidebands, and the loss loop formed by the beating between the ±1st order sidebands and the ±2nd order sidebands at the PD. In fact, there are multiple equivalent feedback loops formed by the RF signals generated by beating between the ±nth order sidebands and the ±(n+1)th order sidebands at the PD. However, the RF signals generated by the beating between the ±nth and ±(n+1)th order sidebands for n larger than 1, have very small amplitudes, which have negligible impact on the PT symmetry of the system. The two beat signals applied to the MZM are combined with a coupling coefficient determined by the Bessel functions of 0th and 2nd order of the first kind. The PT symmetry condition is met at an RF signal frequency f_{RF} when the gain and loss coefficients in the two loops are made equal in magnitude, as shown in Fig. 3. Once the gain/loss coefficient is greater than the coupling coefficient, the PT symmetry is broken and single-frequency oscillation at f_{RF} is achieved.

When microwave oscillation in the OEO loop shown in Fig. 1 is established, the fundamental RF signal photocurrent generated by the beating between the optical carrier with the ±1st order sidebands at the PD can be written as

$$I_{RF,c-1} = -2\Re P_{in}\sin(2\beta_b)J_1(\beta_{RF})J_0(\beta_{RF})\sin(\omega_{RF}t+\varphi_{RF}) \quad (1)$$

where $\Re$ is the responsivity of the PD, P_{in} is the power of the CW light into the MZM, $\beta_b=\pi V_{DC}/V_{\pi,DC}$ is the modulator bias angle introduced by the DC voltage V_{DC} applied to the MZM via the DC port, $V_{\pi,DC}$ is the DC port switching voltage, $J_m(x)$ is the Bessel function of the m^{th} order of the first kind, $\beta_{RF}=\pi V_{RF}/V_{\pi,RF}$ is the modulation index, V_{RF} is the input RF signal voltage, $V_{\pi,RF}$ is the RF port switching voltage, and ω_{RF} and φ_{RF} are the angular frequency and phase of the RF signal produced by the OEO, respectively. Similarly, the fundamental RF signal photocurrent generated by the beating between the ±1st order sidebands with the ±2nd order sidebands at the PD can be written as

$$I_{RF,1-2} = -2\Re P_{in}\sin(2\beta_b)J_1(\beta_{RF})J_2(\beta_{RF})\sin(\omega_{RF}t+\varphi_{RF}) \quad (2)$$

It can be seen from Eqs. (1) and (2), the two fundamental RF signal photocurrents have the same phase, and their amplitudes are proportional to $J_0(\beta_{RF})$ and $J_2(\beta_{RF})$. For β_{RF}<1.84, $J_0(\beta_{RF})$ is larger than $J_2(\beta_{RF})$, and hence $I_{RF,c-1}$ is larger than $I_{RF,1-2}$, and we can make one beat signal experience a net gain and the other experience a net loss. Thus, two equivalent loops with one having a gain and the other a loss are produced. The open loop gains of the two loops are given by

$$G_{RF,c-1}(\omega_{RF}) = \frac{R_{in}I_{RF,c-1}^{\ 2}R_oG_AL_E}{V_{RF}^{\ 2}}H(\omega_{RF}) \quad (3)$$

$$G_{RF,1-2}(\omega_{RF}) = \frac{R_{in}I_{RF,1-2}^{\ 2}R_oG_AL_E}{V_{RF}^{\ 2}}H(\omega_{RF}) \quad (4)$$

where R_{in} is the input resistance of the MZM, R_o is the PD load resistance, G_A is the gain of the EA, L_E is the loss of the electrical components inside the OEO loop, and $H(\omega_{RF})$ is the spectral response of the microwave BPF at ω_{RF}. As can be seen, by controlling the gain G_A of the EA and the power P_{in} of the CW light into the MZM, we can make the gain and loss identical in magnitude, $\log_{10}|G_{RF,c-1}|=-\log_{10}|G_{RF,1-2}|$, to achieve PT symmetry.

According to the coupled mode theory, we have two differential equations describing the interplay between the n^{th} longitudinal modes in the two loops in the time domain [9]

$$\frac{da_n^{(1)}}{dt} = -j\omega_n^{(1)}a_n^{(1)} + j\kappa a_n^{(2)} + g_n a_n^{(1)} \quad (5)$$

$$\frac{da_n^{(2)}}{dt} = -j\omega_n^{(2)}a_n^{(2)} + j\kappa a_n^{(1)} + l_n a_n^{(2)} \quad (6)$$

where $a_n^{(1,2)}$ and $\omega_n^{(1,2)}$ are the amplitudes and the angular frequencies of the n^{th} mode of the gain and loss loops, respectively, $g_n=\ln(\sqrt{G_{RF,c-1}(\omega_n)})\cdot FSR$ and $l_n=\ln(\sqrt{G_{RF,1-2}(\omega_n)})\cdot FSR$ are the gain and loss coefficients of the n^{th} mode of the gain and loss loops, respectively [4]. Each mode has different gain/loss coefficient. κ is the coupling coefficient, which is given by

$$\kappa=\sqrt{\frac{I_{RF,c-1}^{\ 2}}{I_{RF,c-1}^{\ 2}+I_{RF,1-2}^{\ 2}}}FSR \tag{7}$$

The PT symmetry condition is met at a mode denoted by n=0 when g_0=-l_0 [8]. Hence

$$G_{RF,c-1}(\omega_0)\cdot G_{RF,1-2}(\omega_0) = \frac{R_{in}^{\ 2}I_{RF,c-1}^{\ 2}I_{RF,1-2}^{\ 2}R_o^{\ 2}G_A^{\ 2}L_E^{\ 2}H(\omega_0)^2}{V_{RF}^{\ 4}}=1 \tag{8}$$

The eigenfrequencies of the proposed PT symmetric OEO can be obtained by solving Eqs. (5) and (6), which are given by

$$\omega_0^{(1,2)}=\omega_0\pm\sqrt{\kappa^2-\alpha_0^{\ 2}} \tag{9}$$

where α_0=g_0=-l_0. Note that the coupling coefficient and the gain/loss coefficient defined above have a unit of Hz. It can be seen from Eq. (9), when $\alpha_0>\kappa$, a pair of amplifying and decaying modes with the same frequency of $\omega_0^{(1)}=\omega_0^{(2)}=\omega_0=\omega_{RF}$ is generated in the OEO, which is the dominating mode that oscillates in the OEO [5].

Compared with the PT symmetric OEOs implemented in the wavelength space [7] and the polarization space [8], the proposed PT symmetric OEO does not need to use two wavelengths or two polarization states. Although the proposed PT symmetric OEO has a similar structure as the one reported in [8], the operation principle is totally different. In [8], the two equivalent loops were implemented based on polarization division multiplexing. The polarization state of the CW light into the MZM must be accurately tuned to meet the breaking PT symmetry condition. Environmental perturbations that alter the light polarization state would affect the stable operation of the OEO. This problem does not exist in the proposed OEO. In addition, in the proposed OEO, the two equivalent loops share all the components. Thus, environmental perturbations such as temperature change and mechanical vibrations would cause identical changes to the eigenfrequencies in the gain and loss loops. Hence, the PT symmetry condition is always preserved and the OEO has higher operational stability. This is an added advantage compared with the approaches reported in [7] and [8].

An experiment is performed based on the setup shown in Fig. 1 to evaluate the operation of the proposed PT symmetric OEO. A CW light at 1550.12 nm generated by the LD is launched into the MZM with a bandwidth of 40 GHz (Photoline MX-LN-40). The PC is used to adjust the polarization state of the incident light to minimize the polarization dependent loss at the MZM. A 10.1 km long DSF is connected to the output of the MZM. A small fraction (1%) of the optical power after the DSF is coupled out via a 99:1 optical coupler to an optical spectrum analyzer (OSA) for monitoring the system output optical spectrum. The output optical signal after the DSF (99%) is detected by a high-speed PD with a bandwidth of 40 GHz and a responsivity of 0.65 A/W (Finisar XPDV2120R). Two cascaded EAs (Centellax OA3MHQM), each having a gain of around 27 dB at 10 GHz, are connected to the output of the PD to produce a sufficiently high gain. A microwave BPF with a center frequency of 10 GHz and a 3-dB passband width of 20 MHz is connected at the output of the EAs to perform coarse frequency selection. The electrical spectrum and the phase noise of the generated microwave signal are measured by an electrical spectrum analyzer (ESA) (Keysight N9020B) and a signal source analyzer (Keysight E5052B), respectively.

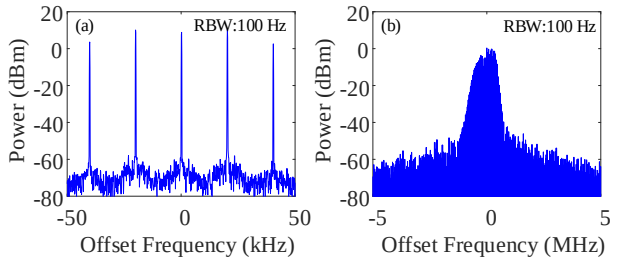

Fig. 4. Multimode oscillation measured by the ESA at a span of (a) 100 kHz and (b) 10 MHz. The spectra are measured at a center frequency of 9.997 GHz.

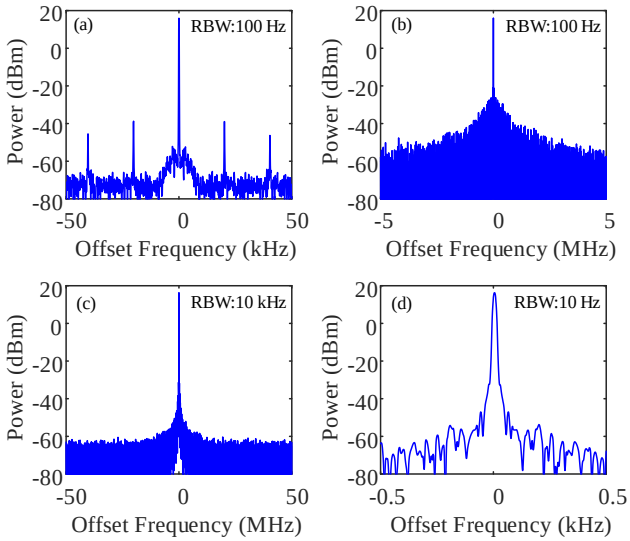

Fig. 5. Single mode oscillation measured by the ESA at a span of (a) 100 kHz, (b) 10 MHz, (c) 100 MHz, and (d) 1 kHz. The spectra are measured at a center frequency of 9.997 GHz.

Firstly, the power of the light from the LD is set to be 13 dBm and the MZM is biased at the quadrature point via a DC power supply. The open loop gain of the gain loop can be obtained by measuring the OEO open loop magnitude response using a vector network analyzer (VNA) connected between the MZM input RF port and the RF splitter output. An open loop gain $G_{RF,c-1}$, which is larger than unity, can be seen at around the microwave BPF passband frequency of 10 GHz. When the OEO loop is closed, oscillation will occur, which can be seen by the spectra shown in Fig. 4(a) and (b). Note that PT symmetry condition is not met at this time, thus multimode oscillation is resulted. As shown in Fig. 4(a), multiple modes are generated and the mode spacing is 20.15 kHz. For the microwave BPF with a 3-dB bandwidth of 20 MHz, there are around 1000 modes within the passband.

Then, we reduce the optical power of the light from the LD by around 3 dB and adjust the MZM bias voltage by a few hundreds of mV away from the quadrature bias voltage to make the breaking PT symmetry condition be satisfied. At this moment, multimode

oscillation is now reduced to single-frequency oscillation, as shown in in Fig. 5(a)-(d), which is measured at four different frequency spans. The sidemodes are 55 dB below the oscillation mode at 9.997 GHz. To evaluate the stability, the system is allowed to operate for 5 hours in a lab environment. No mode hopping is observed during the entire 5-hour measurement period without using a bias controller to stabilize the modulator operating point, which indicates that modulator bias drift has negligible effect on the PT symmetry breaking condition. The oscillation mode has a frequency drift of 28.8 kHz after 5 hours. This is similar to the frequency drift in a conventional OEO [10] and is due to environmental perturbations causing small changes in the OEO loop length. The experimental results confirm that the broken PT symmetry enables the OEO to effectively perform single mode operation. Good long-term stability is also confirmed.

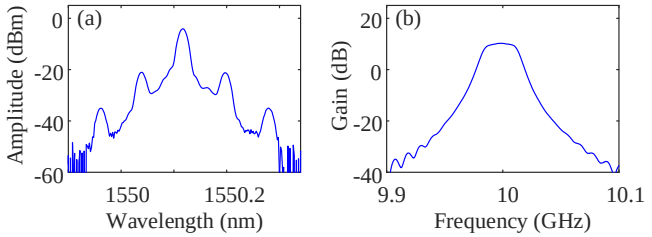

Fig. 6. (a) Optical spectrum when the PT symmetric OEO is oscillating in single mode. (b) Open-loop frequency response of the PT symmetric OEO.

Note that the breaking PT symmetry condition can be verified based on the experiment. Fig. 6(a) shows the optical spectrum when the system is operating in single mode. The modulation index β_{RF} can be estimated based on the power ratio between the optical carrier and the sidebands, which is of 0.45. Substituting β_{RF}=0.45 into Eq. (7), a coupling coefficient κ of 20.13 kHz is calculated. The gain coefficient α_0 can also be obtained from the open loop gain, which is 30.18 kHz. Clearly, the coupling coefficient is smaller than the gain coefficient, the PT symmetry is broken. Fig. 6(b) shows the open-loop gain of the gain loop at around 10 GHz, which is 13 dB. This is larger than the required open-loop gain of 8.7 dB, obtained by substituting β_{RF}=0.45 into Eq. (7) and equating the coupling coefficient and the gain coefficient, to make the system operate above the exceptional point. This confirms that the PT symmetry breaking condition is satisfied. Note that the open loop gain of the loop formed by the beating between the ±2nd order sidebands and the ±3rd order sidebands is proportional to $(J_2(\beta_{RF})J_3(\beta_{RF}))^2$ while the open loop gains of the gain and loss loops are proportional to $(J_0(\beta_{RF})J_1(\beta_{RF}))^2$ and $(J_1(\beta_{RF})J_2(\beta_{RF}))^2$ according to Eqs. (1)-(4). Hence, for β_{RF}=0.45, the values of the open loop gain of the loop formed by the beating between the ±2nd and ±3rd order sidebands is seventh and fourth order of magnitudes smaller than the open-loop gains of the gain and loss loops. Therefore, the effect of the ±3rd and higher order sidebands in the system can be ignored.

The single sideband phase noise of the generated microwave signal when the loop length is 10.1 km is also measured, which is shown by the blue line in Fig. 7. A very low phase noise of around -142 dBc/Hz at a 10 kHz offset frequency is observed. The phase noise of the PT symmetric OEO with a shorter loop length of around 20 m and 1 km are also measured and are shown in Fig. 7 as the red and green lines. They are -86.2 dBc/Hz and -112.7 dBc/Hz at a 10 kHz offset frequency, respectively. As a comparison, the phase noise of a 9.997 GHz microwave signal generated by a commercial microwave signal generator (Analog Devices HMC-T2220) is also shown (as the black line). A phase noise of -97.2 dBc/Hz at 10 kHz can be seen. The phase noise measurements presented in Fig. 7 indicate the proposed PT symmetric OEO with a 1 km loop length has a similar phase noise performance as a commercial microwave signal generator at an offset frequency of less than 1 kHz, and the phase noise performance is 45 dB better than that generated by the commercial microwave signal generator at 10 kHz offset frequency when the loop length is 10.1 km.

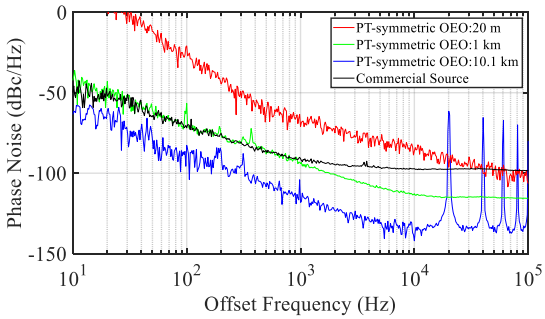

Fig. 7. Phase noise measurements of the microwave signal generated by the PT symmetric OEO with different loop lengths. Phase noise of a microwave signal generated by a commercial microwave signal generator is also shown for comparison.

In conclusion, we have proposed and experimentally demonstrated a new PT symmetric OEO based on higher order modulation. Experimental results showed that the proposed PT symmetric OEO was able to support single-frequency oscillation with a high sidemode suppression ratio of 55 dB. A phase noise as low as -142 dBc/Hz at a 10 kHz offset frequency is demonstrated. At a lab environment, the OEO could stably with no mode hopping being observed for a 5-hour measurement period. The key advantages of the proposed OEO include a simple system configuration and high stability, which make a step closer of OEOs for real world applications.

Funding. Guangdong Province Key Field R&D Program Project under Grant 2020B0101110002; National Natural Science Foundation of China (NSFC) (61860206002, 61771221); National Key R&D Program of China (2021YFB2800804)

Disclosures. The authors declare no conflicts of interest.

Data availability. Data underlying the results presented in this paper are not publicly available at this time but may be obtained from the authors upon reasonable request.

References

1. X. S. Yao and L. Maleki, JOSA B **13**, 1725 (1996).
2. X. S. Yao and L. Maleki, Opt. Lett. **22**, 1867 (1997).
3. K. H. Lee, J. Y. Kim, and W. Y. Choi, IEEE Photon Technol. Lett. **20**, 1645 (2008).
4. L. Li, Y. Cao, Y. Zhi, J. Zhang, Y. Zou, X. Feng, B. O. Guan, and J. Yao, Light Sci. Appl. **9**, 169 (2020).
5. J. Zhang and J. Yao, Sci. Adv., **4,** 6728 (2018).
6. Y. Liu, T. Hao, W. Li, J. Capmany, N. Zhu, and M. Li, Light Sci. Appl. **7**, 38 (2018).
7. J. Zhang, L. Li, G. Wang, X. Feng, B. O. Guan, and J. Yao, Nature Comm. **11**, 3217 (2020).
8. Q. Ding, M. Wang, J. Zhang, Y. Tang, Y. Li, M. Han, Y. Guo, N. Zhang, B. Wu, and F. Yan, APL Photon. **6**, 076102 (2021).
9. H. Hodaei, M. A. Miri, M. Heinrich, D. N. Christodoulides, and M. Khajavikhan, Science **346**, 975 (2014).
10. L. Bogataj, M. Vidmar, and B. Batagelj, J. Light. Technol. **32**, 3690 (2014).

Full references

1. X. S. Yao and L. Maleki, "Optoelectronic microwave oscillator," *JOSA B* **13**(8), 1725-1735 (1996).
2. X. S. Yao and L. Maleki, "Dual microwave and optical oscillator," *Opt. Lett.* **22**(24), 1867-1869 (1997).
3. K. H. Lee, J. Y. Kim, and W. Y. Choi, "Injection-locked hybrid optoelectronic oscillators for single-mode oscillation," *IEEE Photon. Technol. Lett.* **20**(19), 1645-1647 (2008).
4. L. Li, Y. Cao, Y. Zhi, J. Zhang, Y. Zou, X. Feng, B. O. Guan, and J. Yao, "Polarimetric parity-time symmetry in a photonic system," *Light Sci. Appl.* **9,** 169 (2020).
5. J. Zhang and J. Yao, "Parity-time–symmetric optoelectronic oscillator," *Sci. Adv.* **4**(6), 6782 (2018).
6. Y. Liu, T. Hao, W. Li, J. Capmany, N. Zhu, and M. Li, "Observation of parity-time symmetry in microwave photonics," *Light Sci. Appl.* **7**(1), 1-9 (2018).
7. J. Zhang, L. Li, G. Wang, X. Feng, B. O. Guan, and J. Yao, "Parity-time symmetry in wavelength space within a single spatial resonator," *Nature Commun.* **11**(1), 1-7 (2020).
8. Q. Ding, M. Wang, J. Zhang, Y. Tang, Y. Li, M. Han, Y. Guo, N. Zhang, B. Wu, and F. Yan, "Parity-time symmetry in parameter space of polarization," *APL Photon.* **6**(7), 076102 (2021).
9. H. Hodaei, M. A. Miri, M. Heinrich, D. N. Christodoulides, and M. Khajavikhan, "Parity-time–symmetric microring lasers," *Science* **346**(6212), 975-978 (2014).
10. L. Bogataj, M. Vidmar, and B. Batagelj, "A feedback control loop for frequency stabilization in an opto-electronic oscillator," *J. Light. Technol.* **32**(20), 3690-3694 (2014).